

Supplemental material for Strong spin depolarization in the ferromagnetic Weyl semimetal $\text{Co}_3\text{Sn}_2\text{S}_2$: The role of spin-orbit coupling

Sandeep Howlader¹, Surabhi Saha², Ritesh Kumar¹, Vipin Nagpal³, Satyabrata Patnaik³, Tanmoy Das², and Goutam Sheet^{1*}

*¹Department of Physical Sciences, Indian Institute of Science Education and Research
Mohali, Mohali, Punjab, India.*

²Department of Physics, Indian Institute of Science, Bengaluru, Karnataka, India.

³School of Physical Sciences, Jawaharlal Nehru University, Delhi, India

A. Sample preparation technique:

$\text{Co}_3\text{Sn}_2\text{S}_2$ single crystals were synthesized using modified Bridgman method. For polycrystalline $\text{Co}_3\text{Sn}_2\text{S}_2$ stoichiometric amounts of Co lumps (Sigma Aldrich, 99.999%), Sn powder (Sigma Aldrich, 99.999%) and S powder were uniformly mixed in an agate mortar and pelletized. The mixture was then transferred to a vacuum evacuated silica tube. The tube was kept in the furnace for two periods of 48 hrs at 500 °C and 700°C with heating and cooling rate of 0.5°C/min in both the cycles. An intermediate grinding of the samples were to be used. To grow single crystals, the single phase $\text{Co}_3\text{Sn}_2\text{S}_2$ polycrystalline powder was taken in an alumina crucible and again vacuum sealed in a quartz tube. The tube was then slowly heated to 1000°C over 30 hrs, maintained at 1000°C for 24 hrs and slowly cooled to 800°C within 72 hrs. Afterwards, the furnace was turned off and the sample was air quenched to room temperature. Shiny crystals were obtained after cleaving the as-grown ingot with a razor blade. The crystal structure and phase of single crystals were determined from Reitveld refinement of powder X-ray diffraction (shown in Fig.1). Magnetization measurements of single crystals were also carried out at 5 K with applied fields of upto 2 Tesla. The field was applied along the c-axis of the crystal. Saturation magnetization was found to be 0.88 μB/f.u. or $M_s = 0.32 \mu\text{B}/\text{Co}$. The magnetization data is shown in Fig. 1(b).

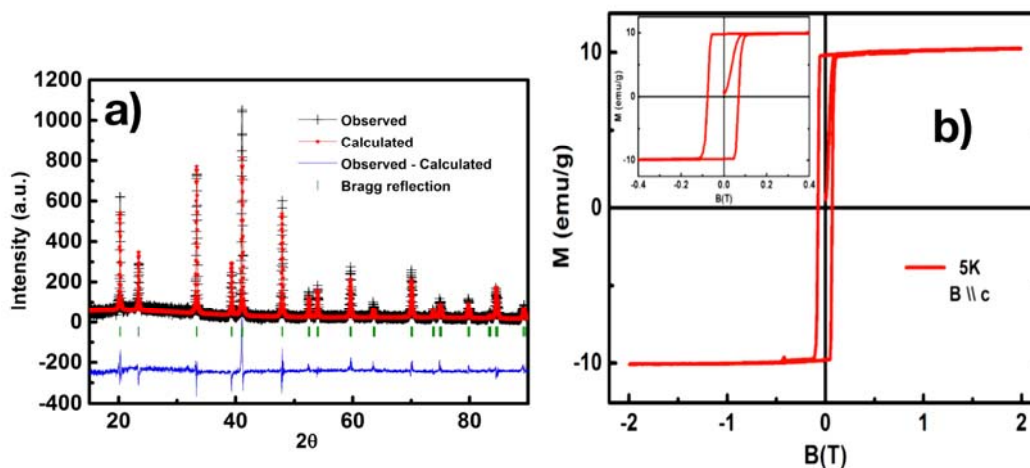


Fig.1. a) Reitveld refinement of powder X-ray diffraction of $\text{Co}_3\text{Sn}_2\text{S}_2$ single crystals. b) Magnetization data obtained for $\text{Co}_3\text{Sn}_2\text{S}_2$ single crystal.

B. Measurement technique:

Point contact spectroscopy is a characterization tool based on four-probe measurement technique. Here, two contacts are drawn from the tip and two from the sample. A lock-in based modulation technique is employed to characterize the sample. A dc current coupled (using an adder circuit) with a small amplitude, low frequency ac current is supplied between the tip and the sample and the potential difference is measured between them using a digital multimeter (dc) and lock-in amplifier (ac). Current through the contact is along z-direction.

The PCS probe utilizes a differential screw arrangement for providing and controlling motion of tip along the z-axis. The probe rests at the center of 3-axis vector magnet where Helmholtz coils enable us to apply 1 Tesla magnetic field along the x or y (in-plane of crystal) direction. And, a solenoidal coil generates upto 6 Tesla magnetic fields along the z direction (c-axis of crystal) (shown in Fig.2).

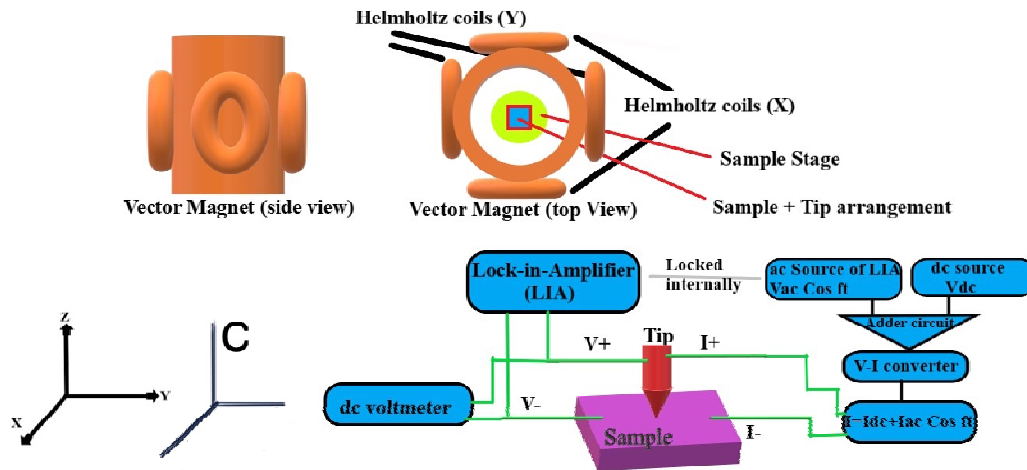


Fig.2. Experimental setup and measurement technique. C-axis of the sample is out of plane. The tip is engaged on the facet perpendicular to the c-axis.

C. Additional experimental data

We now present additional point contact spectroscopic data obtained for a ballistic point contact between Nb/ $\text{Co}_3\text{Sn}_2\text{S}_2$.

a). Asymmetric point contact data

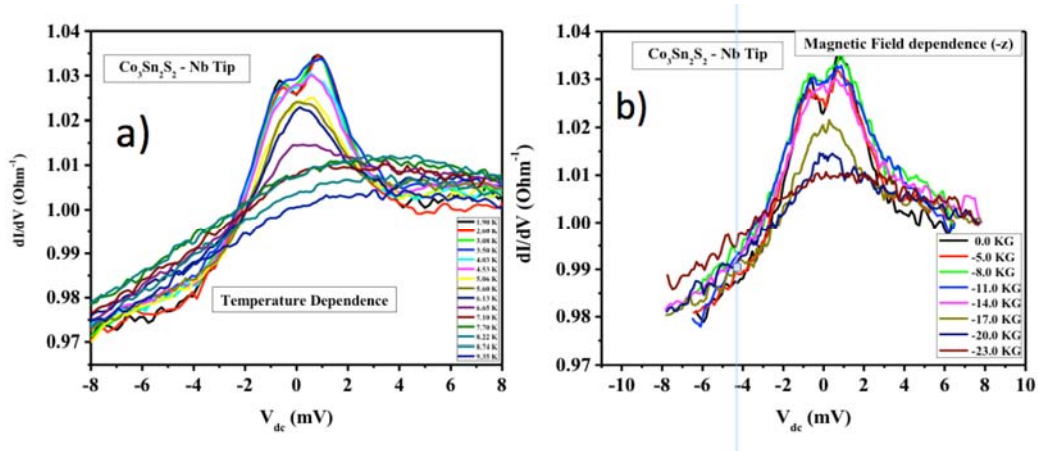


Fig.3. a) Temperature b) magnetic field dependence of point contact spectra obtained for Nb/ $\text{Co}_3\text{Sn}_2\text{S}_2$.

Figure 3. shows spectra obtained for a ballistic point contact. In fig.3(a) we have shown the temperature dependence of the spectra. The spectra is evolving systematically with temperature and disappears at transition temperature. Fig.3(b) shows the magnetic field dependence of the spectra. The spectra evolves systematically and disappears at 23 KG applied along the $-Z$ direction.

b). Extracted Symmetric and Antisymmetric component

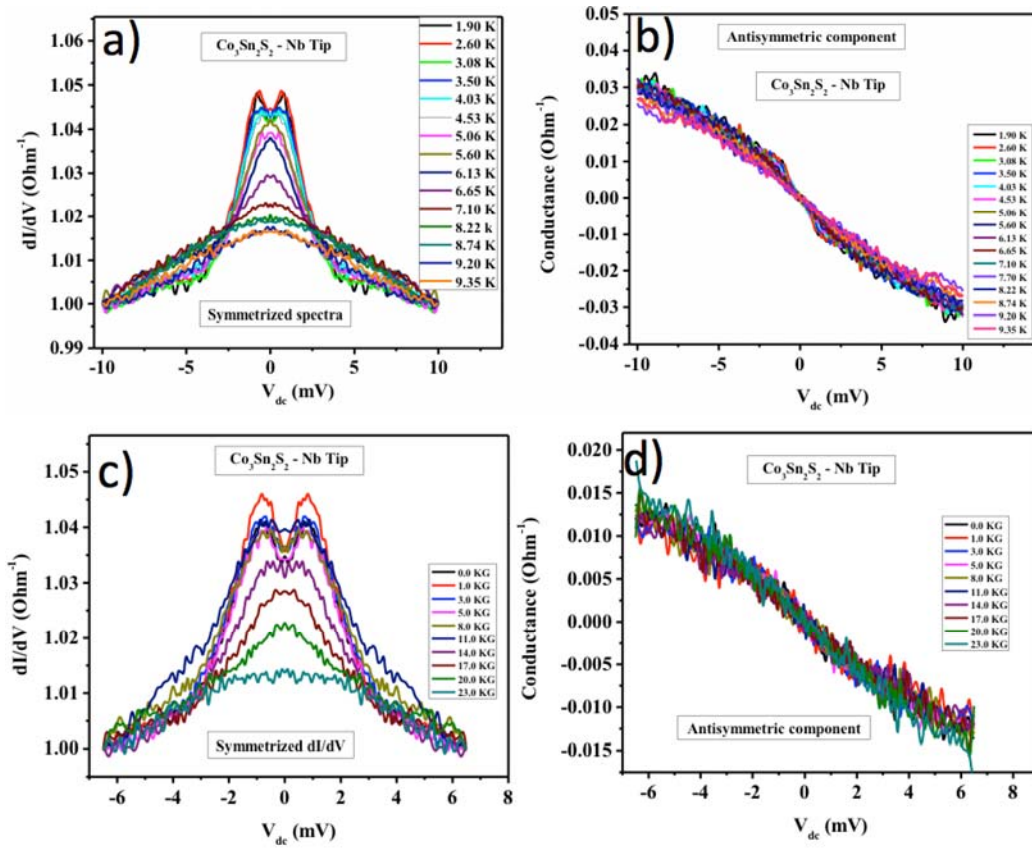


Fig.4. a),c) shows symmetric component of ballistic data respectively b),d) shows antisymmetric component of ballistic data respectively.

The asymmetric ballistic spectra shown in Fig 3. was symmetrized and the symmetric and anti-symmetric components were extracted. Fig. 4 (a),(c) shows the symmetric component of the asymmetric ballistic data and corresponding temperature and magnetic field dependence. In fig.4 (b),(d) we have shown the antisymmetric component derived from the asymmetric spectra and their temperature and magnetic field dependence.

D. Field dependence along the a - b plane.

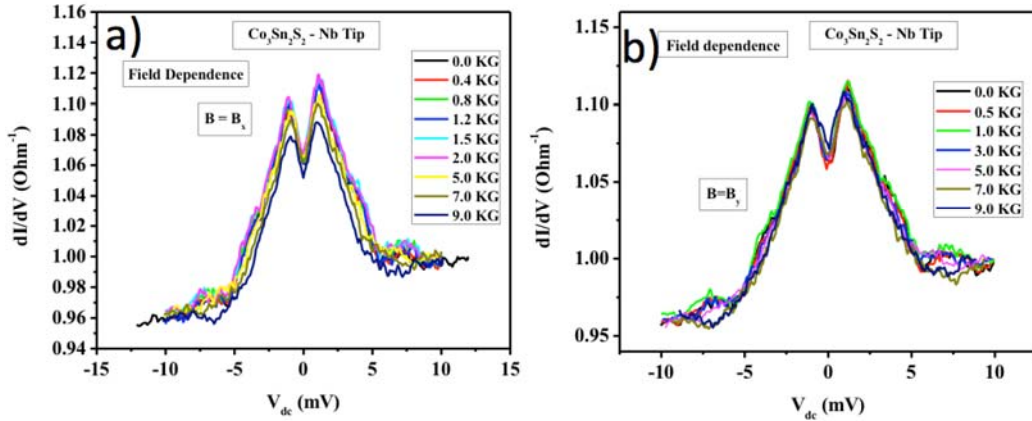


Fig. 5. Magnetic field dependence of ballistic spectra with magnetic field applied along a) X-axis b) Y-axis.

In Fig. 5 we show magnetic field dependence of spectra obtained for a ballistic point contact where field is applied in-plane of the crystal. Application of external magnetic field revealed that the ballistic spectra evolve systematically relatively easily with applied field along the X direction than field applied along Y direction. We are able to apply a maximum of 1 Tesla along the X or Y direction due to instrumental limitations.